Genome-scale modeling of CHO cells unravel the critical role of asparagine in cell culture feed media

Kuin Tian Pang[1,2,3,4#], Yi Fan Hong[1,4,#], Fumi Shouzui[5,#], Shunpei Furomitsu[5], Matthew Myint[1,3], Ying Swan Ho[1], Yaron R. Silberlberg[6], Ian Walsh[1,*], Meiyappan Lakshmanan[1,7,8,9*]

[1]Bioprocessing Technology Institute, Agency for Science, Technology and Research (A*STAR), 20 Biopolis Way, #06-01, Centros 138668, Singapore

[2]Bioinformatics Institute, Agency for Science, Technology and Research (A*STAR), 30 Biopolis Street, #07-01 Matrix, Singapore 138671, Republic of Singapore

[3]Department of Biomedical Engineering, National University of Singapore, 4 Engineering Drive 3 Block 4, #04-08, 117583, Singapore

[4]School of Chemistry, Chemical Engineering and Biotechnology, Nanyang Technological University, 62 Nanyang Drive, N1.2-B3, 637459, Singapore

[5]Biopharma Media Group, Material Development Section, Material & Technology Solution Labs, Research Institute for Bioscience Products & Fine Chemicals, Ajinomoto Co., Inc, 1-1, Suzuki-cho, Kawasaki-ku, Kawasaki-shi, 210-8681, Japan

[6]CELList Solution Centere (CSC), #1403~1405, Songdo AT Center, 70 Songdogwahak-ro, Yeonsu-gu, Incheon, Republic of Korea

[7]Department of Biotechnology, Bhupat and Jyoti Mehta School of Biosciences, Indian Institute of Technology Madras, Chennai 600036, India

[8]Centre for Integrative Biology and Systems medicinE (IBSE), Indian Institute of Technology Madras, Chennai 600036, India

[9]Robert Bosch Centre for Data Science and AI (RBCDSAI), Indian Institute of Technology Madras, Chennai 600036, India

[#] These authors have equally contributed to the work

* Correspondence to: M. Lakshmanan (meiyappan@iitm.ac.in) and I. Walsh (ian_walsh@bti.a-star.edu.sg)

Running Head: Importance of asparagine in CHO feed media

ABSTRACT

Amino acids, including asparagine, aspartate, glutamine, and glutamate, play important roles in purine and pyrimidine biosynthesis as well as serve as anaplerotic sources fueling the tricarboxylic acid (TCA) cycle for mitochondrial energy generation. Despite extensive studies on glutamine and glutamate in CHO cell cultures, the roles of asparagine and aspartate, especially in feed media, remain underexplored. In this study, we utilized the CHO genome scale model to first deeply characterize the intracellular metabolic states of CHO cells cultured in different combinations of basal and feed media to understand the traits of asparagine/aspartate-dependent and glutamate-dependent feeds. Subsequently, we identified the critical role of asparagine and aspartate in the feed media as anaplerotic sources and conducted *in silico* simulations to ascertain their optimal ratios to improve cell culture performance. Finally, based on the model simulations, we reformulated the feed media by tailoring the concentrations of asparagine and aspartate. Our experimental data reveal a CHO cell preference for asparagine compared with aspartate, and thus maintaining an optimal ratio of these amino acids is a key factor for achieving optimal CHO cell culture performance in biopharmaceutical production.

Keywords: mammalian systems biotechnology, Chinese hamster ovary (CHO) cells, genome-scale model (GEM), enzyme capacity constrained flux balance analysis (ecFBA)

1 INTRODUCTION

Chinese hamster ovary (CHO) cells are the most abundantly used expression hosts for the biomanufacturing of recombinant glycoprotein therapeutics due to several advantages including human-like N-glycosylation, ability to grow in suspension culture, and are intrinsically resistant to various virus infections (Walsh, 2018). Since their first use for commercial production in 1980s, the recombinant protein yields from CHO cells have dramatically increased from 100-200 mg/L to more than 7 g/L. Such advancements were achieved through successive development of both high yield and stable cell lines as well as the enhanced process designs (Hong et al., 2018). Almost all the commercial biomanufacturing use a fed-batch process, where the CHO cells are first allowed to rapidly grow and reach a high viable cell density (VCD) and then they are maintained in this state, i.e., stationary phase, during which recombinant protein synthesis reaches the maximum level (Coulet et al., 2022). CHO cells are first cultivated in a chemically defined cell culture basal media which typically contains 40-50 individual components such as nutrients and growth factors to support the unrestricted growth (Ritacco et al., 2018). Comparatively, the feed media, which is predominantly used during the late exponential phase and stationary phase, is less complex and contains mostly primary nutrients such as glucose and amino acids that are required for both CHO cells maintenance and recombinant protein synthesis. Also, excessive feeding of some nutrients could lead to the accumulation of toxic byproducts such as lactate and ammonia in the cell culture, and negatively affect the titer (Rouiller et al., 2013). It is thus vital to carefully optimize both basal and feed media such that only relevant nutrients are supplied in adequate quantities such that overall cell culture performance is enhanced.

Glutamine and asparagine are two key amino acids in animal cell culture media which serve as major energy and nitrogen sources for mammalian cells (Ahn and Antoniewicz, 2013; Jiao et al., 2007; Xu et al., 2014; Zhang et al., 2016). Glutamine is metabolized through glutaminolysis into glutamate which further gets deaminated into alpha-ketoglutarate (α-KG) and enters the tricarboxylic acid (TCA) cycle to generate energy cofactors and biomass

precursors. It has been reported as essential for CHO cell growth as the elimination of glutamine delays the beginning of the exponential growth phase (Duarte et al., 2014). However, since the deamination of glutamine into glutamate releases ammonia, which negatively affects cell growth and recombinant protein synthesis, most of the CHO feed media are devoid of glutamine. Due to glutamine's essentiality, a cell line selection system targeting the glutamine synthetase enzyme, i.e., CHO-GS, is established where the transgene is selected along with the glutamine synthetase gene without glutamine in cell culture media. Similar to glutamine, asparagine is also a key amino acid and consumed in abundant quantities during CHO cell culture (Duarte et al., 2014). Metabolism of asparagine is also very similar to glutamine where asparagine is first deaminated into aspartate and then subsequently transaminated into oxaloacetate to enter the TCA cycle. Deamination of asparagine into aspartate also releases ammonia, and thus has the same effects as glutamine on cell culture. Therefore, to mitigate the ammonia production, the concentrations of glutamine and asparagine are maintained at low levels and typically offset by the higher amounts of glutamate and aspartate, respectively, to ensure the consistent supply of anaplerotic substrates to TCA cycle.

Cell culture media is conventionally designed and optimized through the help of design of experiments (DoE) where the effect of individual components on cell culture performance is evaluated through multivariate statistical analysis (Ritacco et al., 2018). However, these methods rely just on statistical methods which merely correlate the media components and cell culture outputs such as titer in an empirical manner and does not provide any causal relationship between them (Galbraith et al., 2018). It is therefore highly desirable to rationally optimize the media through the systematic characterization of how various media components affect the host's cellular metabolism, which in turn affects cell growth and product yield. In this regard, the availability of high-quality genome-scale models (GEMs) for CHO cells enables the rational characterization of cell culture processes (Park et al., 2024). It has been successfully used to investigate the key bottlenecks in cell culture processes (Calmels et al., 2019; Hong et al., 2020; Selvarasu et al., 2012) and design and optimize media (Hong et al.,

2022; Huang et al., 2020; Savizi et al., 2022; Yeo et al., 2022). Here, we utilize the CHO GEM to first deeply characterize the intracellular metabolic states of CHO cells which were cultivated in multiple combinations of basal and feed media to understand the traits of asparagine/aspartate-dependent and glutamate-dependent feeds. Subsequently, we identify the critical role of asparagine and aspartate in the feed media as anaplerotic sources and conduct hypothetical simulations to ascertain their optimal ratios to improve cell culture performance. Finally, based on the model simulations, we reformulate the feed media by tailoring the concentrations of asparagine and aspartate.

2 MATERIALS AND METHODS

2.1 Cell lines and cultivation

CHO-K1 cell line expressing IgG1 (Ajinomoto Co., Inc., Japan) was used in this study. Fed-batch bioreactor cultures of CHO cells were conducted using Ajinomoto's proprietary CELLiST™ media Basal-A or Basal-B (Ajinomoto Co., Inc., Japan) supplemented with 4 mM glutamine and 50 µg/L LR3-IGF1. Ajinomoto's proprietary feed-a or feed-b were used in combination with Basal-A and Basal-B media for the fed-batch cultures as follows: Basal-A and feed-a (A/a), Basal-A and feed-b (A/b), Basal-B and feed-a (B/a) and Basal-B and feed-b (B/b). The cultures were cultivated until day 15 and 6% of feed was added on days 3, 5, 7, 10 and on 12 if the cell viability was high in all cultures. Glucose was routinely topped-up in all cell cultures to 8 g/L every day from day 3 onwards. Cell culture was conducted in triplicates in Ambr® 15mL microbioreactors (Sartorius, Göttingen, Germany). Temperature of cell culture was controlled at 37°C, dissolved oxygen (DO) control was controlled at 20% and pH was controlled at 7 ± 0.2 by sparging CO_2 gassing or Na_2CO_3 addition. Cell samples and culture supernatants were collected from day 0, and every day from day 2 onwards for biochemical and titer analyses.

2.2 Analytical techniques and biochemical measurements

Viable cell density (VCD) and viability were analyzed by the Vi-Cell XR™ instrument (Beckman Coulter, CA, USA). Concentration of IgG, glucose, lactate, and ammonia were quantified by a Cedex Bio HT analyzer (Roche Custom Biotech, IN, USA). Concentrations of amino acids in supernatants were quantified using Nexera™ Amino Acid Analysis System (Shimadzu, Japan) as per manufacturer's instructions. Concentrations of vitamins, nucleosides and organic acids in supernatants were profiled with LC/MS/MS Method Package for Cell Culture Profiling Ver. 1 (Shimadzu, Japan). Intracellular NAD+ levels were measured using the cell pellets obtained on day 5 and day 7 using a NAD/NADH assay kit (Dojindo, Japan), which allows for the determination of intracellular amounts of total NAD+ and NADH. Similarly, Intracellular ATP concentration on day 5 and day 7 was assessed using a bioluminescence-based ATP Assay Kit (Dojindo, Japan). Both ATP and NAD+ levels were determined by following the protocols provided by the manufacturer.

2.3 Metabolic rates determination

VCD data was fitted with the previously proposed logistic equation (Goudar et al., 2005):

$$X = \frac{A}{e^{Bt} + Ce^{-Dt}}$$

where variables *A*, *B*, *C*, and *D* are positive model parameters, and *X* is the VCD. Logistic equation derived VCD was used in further calculations in place of raw data VCD.

Specific growth rate was estimated by non-linear least squares method with the following equation:

$$\mu' = \frac{\Delta X_v}{\bar{X}_V \Delta t}$$

where μ' is the specific growth rate, X_v is the VCD, and t is time.

Exchange rate equation for q_P and other metabolites were calculated using the method previously proposed (Széliová et al., 2020). q_P across a time segment was estimated by non-linear least squares method with the following equation:

$$qP = \frac{\Delta[P]}{0.5(X_f V_f + X_0 V_0) DCWt}$$

where *[P]* is the product concentration, X_0 is VCD at the initial time point, X_f is VCD at the final time point, V_0 is the volume at initial time point, V_f is the volume at final time point, *DCW* is dry cell weight, and *t* is time.

Exchange rates for glucose, amino acid, lactate, and ammonia q_i was estimated by non-linear least squares method with the following equation:

$$[i] = [i]_0 + \frac{q_i B_0}{\mu}(e^{\mu t} - 1)$$

where $[i]_0$ is metabolite concentration at initial time point, *[i]* is metabolite concentration at final time point, B_0 is biomass, μ is the specific growth rate, and *t* is time.

2.4 Enzyme capacity constrained flux balance analysis (ecFBA)

An updated version of a previously reconstructed CHO GEM with enzyme kinetic parameters was used in this study (Yeo et al., 2020). The newly updated model has 5570 reactions, 2283 genes and 2342 unique metabolites localized across model 7 cellular compartments. The key updates of this unpublished model compared to the previously published one are as follows: (1) inclusion of several di- and tri-peptide metabolic reactions; (2) Correction for glutathione and ATP energetic costs in IgG1 biosynthetic reaction; and (3) Updating of compartment-specific gene reaction associations. A CHO-K1 specific cell line model was subsequently reconstructed by integrating the average CHO-K1 transcriptomics data obtained from literature with this updated CHO GEM. Specifically, transcript abundance data for each gene was pre-processed and binarized as ON and OFF as suggested earlier (Richelle et al., 2019). The binary gene scores were converted to reaction scores by considering multimeric or isozyme relationships as described by the model's gene-protein-relationship matrix in CHO GEM. These binary reaction scores were used as input data for cell line specific model pruning using the mCADRE algorithm (Wang et al., 2012).

Constraint-based flux analysis with additional constraints on enzyme capacity was

used to characterize the metabolic states under various media conditions during the early exponential growth phase (day 2-5) and late growth phases (day 5-8). We chose day 2-5 to analyze the effects of basal media while day 5-8 to analyze the feed media effect. We used an FBA formulation whereby we minimized the overall enzyme usage while simultaneously constraining the measured metabolite uptake/secretion rates, IgG1 specific productivity and specific growth rates. The corresponding optimization problem can be mathematically represented as follows:

$$\min Z_1 = \sum_j \frac{\mathrm{MW}_j v_j}{k_j^{\mathrm{cat}}} \qquad \text{(P1)}$$

Subject to:

$$\sum_j S_{\mathrm{ij}} v_j = 0 \quad \forall i \in M$$

$$\alpha_j \leq v_j \leq \beta_j \forall j \in R$$

where Z is the cellular objective which is the overall cellular enzyme capacity, v_j is the flux through reaction j, M is the list of metabolites, R is the list of reactions, MWj molecular weight of enzymes, k_j^{cat} is the turnover number of enzymes and S_{ij} indicates the stoichiometric coefficient of metabolite i involved in reaction j.

To simulate the physiology of CHO cells, the overall cellular enzyme capacity was minimized while simultaneously constraining the uptake/secretion rates of glucose, lactate, ammonia, IgG, all 20 amino acids and other metabolites at measured values. Note that since the measurements of cysteine and myo-inositol were missing in the experimental data, we allowed the model to freely uptake the desired cysteine and myo-inositol during simulations as these metabolites are essential for cell growth. We used 5000 different permutations in each simulation to account for reactions with unknown k_j^{cat} values and obtained 5000 flux solutions. The geometric mean of the flux solutions surrounding the maxima of the resultant lognormal distributions accurately represent the average cellular state (Bengtsson et al., 2005), and were then used to assess the intracellular flux distribution of the CHO cells.

The geometric mean of flux solutions derived from each ecFBA simulation was used to determine the carbon balance. Particularly, biomass reaction, demand reactions, exchange

reactions, and sink reactions were identified and obtained from the flux solutions. The carbon number of the respective metabolites in identified reactions were multiplied by mean flux value and designated to either carbon input or carbon output.

2.6 Statistical analysis

Data are presented as mean +/- standard error of the mean. Statistical analyses were performed by one-way ANOVA with Fisher's least significant differences (LSD) post hoc test using GraphPad Prism 9 (GraphPad Software Inc., United States). The criterion for significance was $p < 0.05$ ($^{*}p < 0.05$; $^{**}p < 0.01$; $^{***}p < 0.001$; and $^{****}p < 0.0001$).

3 RESULTS

3.1 Characteristics of Ajinomoto CELLiST™ feed media and phenotype profiling CHO cells

Based on the importance of glutamine, glutamate, asparagine and aspartate, two different basal and feed media were developed under the CELLiST™ platform by researchers in Ajinomoto Corporation. While almost all amino acids have comparable concentrations in the two basal media, except that medium B contains higher concentration of three amino acids (alanine ~ 4X, glycine ~ 7X and threonine ~ 2X) (**Figure 1A**). Feed media "feed-a" was markedly different from "feed-b" in terms of amino acid composition. Especially, the concentrations of asparagine (~ 3X), aspartate (~ 2.5X), arginine (~2X) and methionine (~4.5X) were higher in feed-a, while feed-b have significantly higher glutamate (~2X) concentration (**Figure 1B**). It should be highlighted that since the availability of glutamine in mammalian cell culture media leads to significant ammonia accumulation, both the basal and feed media were devoid of it although it is recommended to supplement glutamine at the beginning of cell culture. Since glutamine/glutamate and asparagaine/aspartate supply anaplerotic substrates and serve as energy sources, feed-a and feed-b shall be classified as asparagine/aspartate-dependent and glutamate-dependent feeds respectively.

In this work, we aim to assess the performance of the asparagine/aspartate-dependent and glutamate-dependent feeds and understand the criticality of these amino acids in the absence of glutamine. To do so, 14-day fed-batch ambr® 15mL microbioreactor cultures of a IgG1-producing CHO-K1 cell line were performed in two basal and feed media combinations in biological triplicates. In all cell cultures, days 2 - 6 was considered as exponential growth phase with all cultures achieving the highest growth rates at their respective culture conditions. Stationary phase occurred between days 6 – 11 during which the cultures maintained steady growth and cell viability. Death phase was assigned to cultures after day 11 when both viable cell density and viability began to decline. Growth profiles of all four cultures showed significant differences: Basal-A/feed-a combination resulted in best performance with peak viable cell densities (VCD) at 2.58×10^6 cells/mL while Basal-B/feed-b combination had the least performance with peak VCD at 1.81×10^6 cells/mL (**Figure 1C**). Cell cultures cultivated in Basal-B medium displayed slower cell doublings than Basal-A in the initial exponential growth phases. As cell cultures progressed, cell cultures fed with feed-a showed better VCD than feed-b. While VCD displayed significant differences, no major difference in cell viability was observed across different media combinations until day 12 (**Figure 1D**). In terms of IgG1 productivity, feed-a containing cell cultures showed the best performance with a maximum titer of 8.3 g/L, while feed-b containing cell cultures reached a maximum titer of only 7.3 g/L (**Figure 1E**).

To quantitatively assess the differences in cell growth, we calculated the specific growth rates using the logistic equation fitted to VCD. While Basal-A media supports marginally higher growth rates in the initial cell culture days, feed-a containing media showed higher specific growth rates than feed-b containing media from day 5 onwards (**Figure 2A**). No appreciable difference in IgG specific production rate in initial culture days was observed. From day 3 onwards, feed-a containing media supported higher product synthesis than feed-b (**Figure 2B**).

Daily glucose, lactate, ammonia, and amino acids concentrations were also obtained throughout the 14-day microbioreactor cultures and used to calculate consumption or

production rates across culture growth phases over different day segments. Glucose concentrations and specific consumption rates (**Figure 2C**) were comparable regardless of different media combinations. However, lactate production rates in basal-B containing media trended higher than those of basal-A media in early growth phase. Conversely, lactate consumption rates were higher in basal-B containing media compared with those of basal-A counterparts (**Figure 2D**). Ammonium secretion was observed to be significantly high in feed-a containing cultures than that of feed-b (**Figure 2E**).

We then compared the amino acid uptake or secretion rates between the different media combinations in early exponential growth phase (day 2 - 5). Similar to the ammonia secretion patterns, amino acid consumption revealed feed media-dependent patterns which is akin to their initial amino acid compositions discussed earlier: uptake of both asparagine and aspartate was markedly higher in feed-a, i.e., A/a and B/a, than that of feed-b, i.e., A/b and B/b. Feed-b containing cell cultures, on the other hand, consumed glutamate multiple folds higher than feed-a consistent with the initial concentration in the two media. Moreover, the uptakes of arginine, histidine, methionine and proline were also higher in feed-a than feed-b cell cultures (**Figure 3A**). Overall, these trends indicate that CHO cells differentially consume various amino acids as per the initial composition of the feed media, which in turn could contribute to the feed-media dependent phenotypic differences. Between day 5 and 8, similar trends were also observed. Amino acid uptake or secretion rates during this period mirror those seen in the earlier day segments. Notably, the feed media-dependent persists, reaffirming the influence of initial amino acid compositions (**Figure 3B)**.

3.2 ecFBA of CHO GEM highlights differential carbon allocation in a feed-specific manner

To understand intracellular metabolic events, enzyme capacity constrained flux balance analysis (ecFBA) was conducted on the CHO model (Yeo et al., 2020) using the uptake/secretion rates from days 2-5 and days 5-8. It should be highlighted that we

implemented ecFBA over conventional FBA as we have previously shown its superior ability to predict the intracellular flux predictions more accurate than other constraint-based approaches such as pFBA and FBA (Yeo et al., 2020). Resultant metabolic flux distributions among all media combinations (A/a, A/b, B/a and B/b) were compared to identify distinctive metabolic features upon different media. While the flux through glycolysis and pentose phosphate pathway (PPP) did not display notable changes, fluxes through tricarboxylic acid (TCA) cycle and the flux entry points into TCA cycle via aspartate/oxaloacetate and glutamate/α-ketoglutarate showed feed dependent behavior (**Figure 4A**). Higher fluxes through these pathways were observed in A/a and B/a than that of A/b and B/b. We further used the model simulations to compare the overall carbon balance in each condition and calculate how cells consume and distribute carbon element from nutrients into biomass, IgG1, metabolite secretion and CO_2. Overall, cultures with basal media Basal-A assimilated more carbon than Basal-B (~2.8 C-mol vs 2.65 C-mol) (data not shown). While the carbon from glucose consumption was similar across all conditions, carbon from amino acids was marginally higher in feed-a containing cultures (data not shown). In terms of carbon distribution, the allocation of carbon to IgG is very similar across all conditions. However, biomass synthesis was feed dependent: Feed-a containing cell cultures resulted in similar biomass ~30% but feed-b showed greater differences (27% vs 32%) depending on the basal media used. On the other hand, lactate, alanine and glycine secretion were basal media dependent, where all these metabolites were secreted in high amounts in Basal-A media. Overall, these observations indicated that during the cell culture phase between days 2 and 5, the effect of basal media was diminished, and the effect of feed media started to reveal. Analysis of total carbon uptake and secretion between days 5 and 8 indicated that feed-a containing cultures assimilated more carbon than feed-b (~2 C-mol vs 1.95 C-mol) (data not shown**)**. In terms of glucose, a clear pattern was observed: A/a>A/b>B/a>B/b (**Figure 4B**). Similarly, feed-a containing cell cultures allocated more carbon towards IgG1 and biomass synthesis (**Figure 4C**). Particularly, biomass synthesis showed appreciable differences. Feed-a containing cell cultures allocated ~17.4% of total carbon towards biomass synthesis while

feed-b allocated only half of that (~13.8%). Less amounts of wasteful metabolites such as organic acids were secreted in feed-a containing cell cultures when compared to feed-b (10.4% vs 15.9%) (**Figure 4C**).

3.3 Asparagine/aspartate dependent feed results in higher redox cofactors through a balanced TCA cycle flux

Since feed-a resulted in better culture performance in terms of growth and IgG1 specific productivity regardless of basal media used, internal metabolic fluxes between feed-a and feed-b in both basal-A and basal-B were compared to identify feed media specific effects. We noted that titer differences between feed-a and feed-b were predominantly due to differences in energy metabolism and cell growth. Basically, mitochondrial ATP synthesis and NAD/NADH turnover rates were higher in cell cultures supplemented with feed-a when compared to that of feed-b (**Figure 4D-E**). A significant increase in mitochondrial ATP synthase (ATPS4) was observed in feed-a than feed-b, contributing to increased ATP synthesis in the former. In terms of NAD/NADH turnover, the contributions of glyceraldehyde-3-phosphate dehydrogenase (GAPD) from glycolysis were comparably higher in feed-a conditions than feed-b. Such elevated glycolytic flux can be supported in feed-a conditions possibly because of their higher ability to recycle the NAD. We noted that carbon influx entered the TCA cycle at two nodes in feed-a containing cell cultures: oxaloacetate (OAA) via asparagine/aspartate and glutamate. The high amounts of asparagine and aspartate in feed-a were increasingly metabolized by asparaginase (ASNN) and aspartate transaminase (ASPTA) reactions. Importantly, ASPTA supplied OAA to the TCA cycle, which was also strongly replenished by both MDH and pyruvate carboxylase reactions (respective malate → OAA and pyruvate → OAA fluxes). Part of carbon flux from ASPTA also entered the TCA cycle via glutamate and α-ketoglutarate (α-KG). On the other hand, feed-b containing cell cultures showed that carbon flux dominantly entered the TCA cycle from a single entry-point: via glutamate and α-KG (**Figure 4F**). Here, it should be noted that earlier Martinez et al. have noted that the MDH flux could be the

bottleneck in TCA cycle replenishment in CHO cells (Martínez et al., 2013), which is being effectively addressed in feed-a based on the elevated concentrations of asparagine and aspartate. To further confirm this model simulated intracellular flux behavior, we measured the intracellular ATP and NAD+ concentrations on day 5 and 7 and compared the change in concentrations between day 5 and day 7 in all four conditions, i.e. ΔATP and ΔNAD+. These experiments confirmed that while intracellular ATP levels significantly increased from day 5 to 7 in A/a and B/a conditions but remained almost same in A/b and B/b conditions (**Figure 4F**). We also noted a potential similar increase in intracellular NAD+ levels from day 5 to 7 in A/a and B/a conditions but not in B/a and B/b conditions (**Figure 4G**). Together, based on our *in silico* simulations and experimental measurements, we conclude that the difference in flux distribution in and around TCA cycle contributed to the higher redox cofactor regeneration via more balanced TCA cycle flux in feed-a containing cell cultures and thus contributed to improved cell growth and titer.

3.4 Rebalancing of asparagine but not aspartate concentration improves performance of glutamate-dependent feed

As feed-b resulted in poorer culture performance in terms of both growth and IgG1 specific productivity, regardless of basal media used, we further investigated the role of asparagine and aspartate as anaplerotic sources in addition to glutamate in this feed media. Since both asparagine and aspartate can contribute to the TCA cycle flux via oxaloacetate, it may be ideal to use higher amounts of aspartate in the feed than asparagine as it is well known that excess asparagine leads to ammonia accumulation. However, feed-a contained slightly higher amounts of asparagine than aspartate (Asn/Asp ratio of ~1.5). Therefore, we evaluated *in silico* whether increasing either aspartate or asparagine in feed shall improve the cell culture or should we specifically maintain higher Asn/Asp ratio. We performed newer simulations by changing the uptake rates of either asparagine or aspartate individually such that it reflects different Asn/Asp ratios, i.e. 0.5, 0.7, 3 and 4.5, and evaluated its effect on specific growth rate

and IgG1 specific productivity (see Methods). These simulations indicated that increasing of either asparagine or aspartate uptake rates individually, irrespective of the asparagine to aspartate (Asn/Asp) ratios, had a positive effect on specific growth rate while no change was observed on the IgG1 (**Figure 5A**). Further, analysis of *in silico* simulations indicated that the excess supply of either aspartate or asparagine resulted in higher ATP synthesis through TCA cycle and oxidative phosphorylation.

In order to verify the simulation results, another round of cell culture was done using Basal-A medium with feed-b (Asn/Asp – 1.5) and the modified combinations of feed-b where we particularly topped up the concentrations of aspartate or asparagine reflecting different Asp/Asn ratios: 2x Asn feed-b (Asn/Asp – 3), 3x Asn feed-b (Asn/Asp – 4.5), 2x Asp feed-b (Asn/Asp – 0.7), 3x Asp feed-b (Asn/Asp – 0.5). From these experiments, while we observed considerable increase in the VCD and titer when there is an increase in asparagine concentration, i.e. 2x Asn feed-b (Asn/Asp – 3), 3x Asn feed-b (Asn/Asp – 4.5), no major difference was observed when aspartate concentration was increased (**Figure 5B-D**). This observed phenotype is not in full agreement with the simulations as we noted an increase in VCD and titer upon increasing the concentration of asparagine or aspartate, which we thought could be attributed to the ability of cells to uptake individual amino acids. We explored the correlation between the distribution of amino acid concentration in spent media and the corresponding uptake rate (**Figure 5E** and **Figure 5F**) and noted that the aspartate uptake rate showed a plateauing trend with any increase of the concentration above 5mM while asparagine showed a strong linear trend within the recorded range of metabolite concentration. This suggest that even though there is no major difference in terms of asparagine or aspartate metabolism intracellularly, CHO cells do not consume aspartate over a certain extracellular concentration while asparagine is readily consumed as the extracellular concentration increases. It is known that the consumption of aspartate is followed by the utilization of asparagine. Aspartate is transported into cells via glutamate transporters, known as System X^-_{AG} (Kastelic et al., 2019), in conjunction with the cotransport of three Na^+ ions and one H^+ ion, as well as the countertransport of a single K^+ ion (Kanai et al., 2004). The

concentration of intracellular K^+ is regulated by the Na^+/K^+ ATPase, which is associated with ATP degradation. Consequently, it is hypothesized that the uptake of aspartate indirectly results in ATP consumption. In contrast, System N transporters, which facilitate asparagine transport, do not necessitate the efflux of K^+ ions, but solely H^+ ions. This indicates that asparagine may be the preferred substrate in terms of intracellular energy balance, explaining why the rate of asparagine uptake rapidly increases with its concentration unlike aspartate. Moreover, as the asparagine concentration in feed increases, it leads to higher amount of ammonia production which is often suggested to hinder cell growth when it exceeds concentration of 5mM (Kyriakopoulos and Kontoravdi, 2014). However, we did not observe such ammonia toxicity as all the four conditions had ammonia levels exceeding >5 mM, particularly, A/a and B/a which has high amounts of asparagine resulted in ammonia levels >7 mM.

Overall, this suggests that a higher Asn/Asp ratio in the feed media is required (preferably around 3) to have a favorable cellular metabolism in CHO cells that could result in an enhanced titer.

4 CONCLUDING REMARKS

Asparagine, aspartate, glutamine and glutamate serve as key nitrogen sources in mammalian cell cultures as they are not only required for de novo purine and pyrimidine synthesis, but also serve as anaplerotic sources fueling TCA cycle for ATP generation (Ahn & Antoniewicz, 2013; Dean and Reddy, 2013; Fomina-Yadlin et al., 2014; Zhang et al., 2016). While the role of glutamine and glutamate in CHO cell cultures has been extensively evaluated, the role of asparagine and aspartate have not been explored fully, particularly in the feed media. In this work, we explored the role of these amino acids using two different feed media (both of which are free from glutamine), where one is fortified with glutamate and the other with asparagine and aspartate. Our study revealed that the feed with higher amounts of asparagine and aspartate than glutamate achieved balanced supply of anaplerotic sources to the TCA cycle,

which in turn resulted in higher VCD and titer. This observation is highly consistent with the earlier study which also reported that asparagine is crucial than glutamine in terms of achieving higher VCD and titer through enhanced energy metabolism and reduced lactate production (Zhang et al., 2016). On the other hand, a recent study showed that while glutamine remains a preferred nitrogen source during exponential growth phase, asparagine can be a secondary source in the absence of glutamine (Kirsch et al., 2022). Despite the criticality of asparagine and glutamine, excessive consumption of either of these amino acids are undesirable for cell culture performance as the metabolism of either of these amino acids lead to significant ammonia accumulation in the culture. Therefore, we also evaluated the possibility of replacing aspartate with asparagine in the feed with different Asn/Asn ratios. Interestingly, while our simulations indicated that increasing either aspartate or asparagine consumption showed similar ability to fuel TCA cycle and thereby improving VCD and titer, experiments showed the preference of CHO cells to consume asparagine over aspartate, and thus performing better in higher asparagine feeds. Overall, our study revealed that maintaining a Asn/Asp ratio of around 3 would be beneficial for CHO cell cultures to achieve optimal performance.

Acknowledgements

This work is supported by the funding from Biomedical Research Council of A*STAR (Agency for Science, Technology and Research), Singapore, and Ajinomoto Corporation (through industry collaboration project ID: SC17/21-304412). This research is also supported by A*STAR Career Development Funds (C210112057).

Conflict of interest

The authors declare that there are no conflicts of interest.

References

Ahn WS, Antoniewicz MR. 2013. Parallel labeling experiments with [1,2-(13)C]glucose and [U-(13)C]glutamine provide new insights into CHO cell metabolism. *Metab. Eng.* **15**:34–47.

Bengtsson M, Ståhlberg A, Rorsman P, Kubista M. 2005. Gene expression profiling in single cells from the pancreatic islets of Langerhans reveals lognormal distribution of mRNA levels. *Genome Res.* **15**:1388–1392.

Calmels C, McCann A, Malphettes L, Andersen MR. 2019. Application of a curated genome-scale metabolic model of CHO DG44 to an industrial fed-batch process. *Metab. Eng.* **51**:9–19.

Coulet M, Kepp O, Kroemer G, Basmaciogullari S. 2022. Metabolic Profiling of CHO Cells during the Production of Biotherapeutics. *Cells* **11**:1929. https://www.mdpi.com/2073-4409/11/12/1929/htm.

Dean, J., & Reddy, P. (2013). Metabolic analysis of antibody producing CHO cells in fed-batch production. *Biotechnology and Bioengineering*, *110*(6), 1735–1747. https://doi.org/10.1002/bit.24826

Duarte TM, Carinhas N, Barreiro LC, Carrondo MJT, Alves PM, Teixeira AP. 2014. Metabolic responses of CHO cells to limitation of key amino acids. *Biotechnol. Bioeng.* **111**:2095–106.

Fomina-Yadlin, D., Gosink, J. J., McCoy, R., Follstad, B., Morris, A., Russell, C. B., & McGrew, J. T. (2014). Cellular responses to individual amino-acid depletion in antibody-expressing and parental CHO cell lines. *Biotechnology and Bioengineering*, *111*(5), 965–979. https://doi.org/10.1002/bit.25155

Galbraith SC, Bhatia H, Liu H, Yoon S. 2018. Media formulation optimization: current and future opportunities. *Curr. Opin. Chem. Eng.* **22**:42–47. https://doi.org/10.1016/j.coche.2018.08.004.

Goudar CT, Joeris K, Konstantinov KB, Piret JM. 2005. Logistic equations effectively model

mammalian cell batch and fed-batch kinetics by logically constraining the fit. *Biotechnol. Prog.* **21**:1109–1118.

Hayter PM, Curling EM, Baines AJ, Jenkins N, Salmon I, Strange PG, Bull AT. 1991. Chinese hamster ovary cell growth and interferon production kinetics in stirred batch culture. *Applied Microbiology and Biotechnology*. 34(5):559-64. doi: 10.1007/BF00167898. PMID: 1367524.

Hong JK, Yeo HC, Lakshmanan M, Han S-H, Cha HM, Han M, Lee D-Y. 2020. In silico model-based characterization of metabolic response to harsh sparging stress in fed-batch CHO cell cultures. *J. Biotechnol.* **308**.

Hong JK, Choi DH, Park SY, Silberberg YR, Shozui F, Nakamura E, Kayahara T, Lee DY. 2022. Data-driven and model-guided systematic framework for media development in CHO cell culture. *Metab. Eng.* **73**:114–123. https://doi.org/10.1016/j.ymben.2022.07.003.

Hong JK, Lakshmanan M, Lee D-Y. 2018. Towards next generation CHO cell line development and engineering by systems approaches. *Curr. Opin. Chem. Eng.* **22**:1–10.

Huang Z, Xu J, Yongky A, Morris CS, Polanco AL, Reily M, Borys MC, Li ZJ, Yoon S. 2020. CHO cell productivity improvement by genome-scale modeling and pathway analysis: Application to feed supplements. *Biochem. Eng. J.* **160**:107638. https://doi.org/10.1016/j.bej.2020.107638.

Jiao Y, Lau OS, Deng XW. 2007. Light-regulated transcriptional networks in higher plants. *Nat. Rev. Genet.* **8**:217–30. http://www.ncbi.nlm.nih.gov/pubmed/17304247.

Kanai, Y. and Hediger, M.A., 2004. The glutamate/neutral amino acid transporter family SLC1: molecular, physiological and pharmacological aspects. Pflügers Archiv, 447, pp.469-479. http://doi.org/10.1007/s00424-003-1146-4 471

Kastelic, M., Kopač, D., Novak, U. and Likozar, B., 2019. Dynamic metabolic network modeling of mammalian Chinese hamster ovary (CHO) cell cultures with continuous phase kinetics transitions. Biochemical Engineering Journal, 142, pp.124-134. https://doi.org/10.1016/j.bej.2018.11.015

Kirsch, B. J., Bennun, S. V., Mendez, A., Johnson, A. S., Wang, H., Qiu, H., Li, N., Lawrence,

S. M., Bak, H., & Betenbaugh, M. J. (2022). Metabolic analysis of the asparagine and glutamine dynamics in an industrial Chinese hamster ovary fed-batch process. *Biotechnology and Bioengineering*, *119*(3), 807–819. https://doi.org/10.1002/bit.27993

Kyriakopoulos S, Kontoravdi C. 2014. A framework for the systematic design of fed-batch strategies in mammalian cell culture. *Biotechnology and Bioengineering*. 111(12):2466-76. doi: 10.1002/bit.25319.

Maddocks ODK, Labuschagne CF, Adams PD, Vousden KH. 2016. Serine Metabolism Supports the Methionine Cycle and DNA/RNA Methylation through De Novo ATP Synthesis in Cancer Cells. *Mol. Cell* **61**:210. /pmc/articles/PMC4728077/.

Martínez, V.S., Dietmair, S., Quek, L.E., Hodson, M.P., Gray, P. and Nielsen, L.K., 2013. Flux balance analysis of CHO cells before and after a metabolic switch from lactate production to consumption. Biotechnology and bioengineering, 110(2), pp.660-666. doi.org/10.1002/bit.24728

Park SY, Choi DH, Song J, Lakshmanan M, Richelle A, Yoon S, Kontoravdi C, Lewis NE, Lee DY. 2024. Driving towards digital biomanufacturing by CHO genome-scale models. *Trends in Biotechnology*. doi: 10.1016/j.tibtech.2024.03.001. Epub ahead of print.

Richelle A, Joshi C, Lewis NE. 2019. Assessing key decisions for transcriptomic data integration in biochemical networks. *PLOS Comput. Biol.* **15**:e1007185. https://journals.plos.org/ploscompbiol/article?id=10.1371/journal.pcbi.1007185.

Ritacco F V., Wu Y, Khetan A. 2018. Cell culture media for recombinant protein expression in Chinese hamster ovary (CHO) cells: History, key components, and optimization strategies. *Biotechnol. Prog.* **34**:1407–1426.

Rouiller Y, Périlleux A, Collet N, Jordan M, Stettler M, Broly H. 2013. A high-throughput media design approach for high performance mammalian fed-batch cultures. *MAbs* **5**:501–511.

Savizi ISP, Maghsoudi N, Motamedian E, Lewis NE, Shojaosadati SA. 2022. Valine feeding reduces ammonia production through rearrangement of metabolic fluxes in central carbon metabolism of CHO cells. *Appl. Microbiol. Biotechnol.* **106**:1113–1126. https://link.springer.com/article/10.1007/s00253-021-11755-4.

Selvarasu S, Ho YS, Chong WPK, Wong NSC, Yusufi FNK, Lee YY, Yap MGS, Lee D-Y. 2012. Combined in silico modeling and metabolomics analysis to characterize fed-batch CHO cell culture. *Biotechnol. Bioeng.* **109**:1415–29. http://www.ncbi.nlm.nih.gov/pubmed/22252269.

Széliová D, Ruckerbauer DE, Galleguillos SN, Petersen LB, Natter K, Hanscho M, Troyer C, Causon T, Schoeny H, Christensen HB, Lee DY, Lewis NE, Koellensperger G, Hann S, Nielsen LK, Borth N, Zanghellini J. 2020. What CHO is made of: Variations in the biomass composition of Chinese hamster ovary cell lines. *Metab. Eng.* **61**:288–300.

Walsh G. 2018. Biopharmaceutical benchmarks 2018. *Nat. Biotechnol.* **36**:1136–1145. http://dx.doi.org/10.1038/nbt.4305.

Wang Y, Eddy J a, Price ND. 2012. Reconstruction of genome-scale metabolic models for 126 human tissues using mCADRE. *BMC Syst. Biol.* **6**:153. http://www.pubmedcentral.nih.gov/articlerender.fcgi?artid=3576361&tool=pmcentrez&rendertype=abstract.

Wurm FM, Hacker D. 2011. First CHO genome. *Nat. Biotechnol.* **29**:718–720. http://dx.doi.org/10.1038/nbt.1943.

Xu P, Dai XP, Graf E, Martel R, Russell R. 2014. Effects of glutamine and asparagine on recombinant antibody production using CHO-GS cell lines. *Biotechnol. Prog.* **30**:1457–1468. https://onlinelibrary-wiley-com.ejproxy.a-star.edu.sg/doi/full/10.1002/btpr.1957.

Yeo HC, Hong JK, Lakshmanan M, Lee D-Y. 2020. Enzyme capacity-based genome scale modelling of CHO cells. *Metab. Eng.* **60**:138–147. https://doi.org/10.1101/2019.12.19.883652.

Yeo HC, Park SY, Tan T, Ng SK, Lakshmanan M, Lee DY. 2022. Combined multivariate statistical and flux balance analyses uncover media bottlenecks to the growth and productivity of Chinese hamster ovary cell cultures. *Biotechnol. Bioeng.* **119**:1740–1754.

Zhang L xiang, Zhang W yan, Wang C, Liu J tao, Deng X cun, Liu X ping, Fan L, Tan W song. 2016. Responses of CHO-DHFR cells to ratio of asparagine to glutamine in feed media: cell growth, antibody production, metabolic waste, glutamate, and energy metabolism.

566 *Bioresour. Bioprocess.* **3**:5.

567

Figure Legends

Figure 1. **Characteristics of CELList media and CHO cell phenotype observed in this media.** Amino acid concentration in basal (A) and feed (B) media. CHO cell viable cell density (VCD) (C) and viability (C), IgG titer (D), glucose (E), and lactate (F) concentration measured in various media combinations of basal and feed media. A/a – Basal A + Feed A; A/b – Basal A + Feed B; B/a – Basal B + Feed A; B/b – Basal B + Feed B. [shaded area denotes ± 1 standard error]

Figure 2. **(A) Specific growth rate, (B) IgG biosynthesis rate and uptake/secretion rates of (C) glucose, (D) lactate, and (E) ammonia between different day segments.** [One-way ANOVA followed by Fisher's LSD post hoc test; ∗p < 0.05; ∗∗p < 0.01; ∗∗∗p < 0.001; and ****p < 0.0001]

Figure 3. Uptake/secretion rates of 20 amino acids across two different time segments – (A) between day 2 – 5, and (B) day 5 – 8. [One-way ANOVA followed by Fisher's LSD post hoc test; ∗p < 0.05; ∗∗p < 0.01; ∗∗∗p < 0.001; and ****p < 0.0001]

Figure 4. (A) Metabolic flux map, simulated (B) carbon input from media, (C) carbon output, (D) ATP production, (E) and NAD production of CHO cells cultured in various media combinations between day 5 - 8. (F) Difference in (F) ATP and (G) NAD+ were measured experimentally between day 5-7. [One-way ANOVA followed by Fisher's LSD post hoc test; ∗p < 0.05; ∗∗p < 0.01]

Figure 5. In-silico simulation suggest that Increased asparagine and aspartate in culture are predicted to have higher (A) relative performance of cell culture. Experimental validation of increased asparagine and aspartate in culture showed that double asparagine significantly improved (B) VCD [while maintaining viability] and (C) IgG titer, compared with control A/b media combination and doubled aspartate in media. Correlation analysis reveals that CHO cell exchange rate has better correlation with concentration of (D) asparagine, compared with (E aspartate. [shaded area denotes ± 1 standard error]

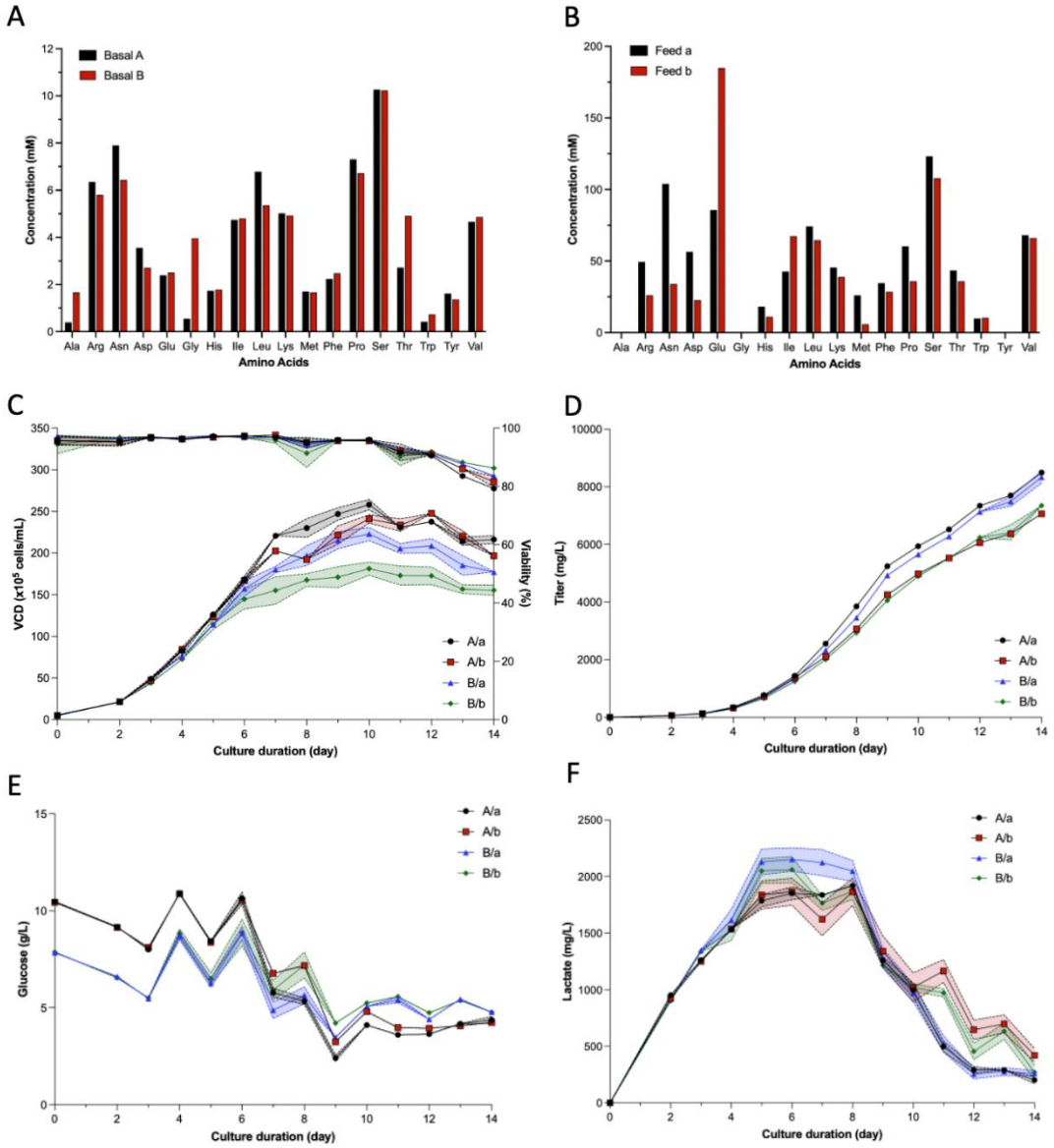
A
Basal A
Basal B
Concentration (mM)
Ala Arg Asn Asp Glu Gly His Ile Leu Lys Met Phe Pro Ser Thr Trp Tyr Val
Amino Acids
B
Feed a
Feed b
Concentration (mM)
Ala Arg Asn Asp Glu Gly His Ile Leu Lys Met Phe Pro Ser Thr Trp Tyr Val
Amino Acids
C
VCD (x10^5 cells/mL)
Viability (%)
A/a
A/b
B/a
B/b
Culture duration (day)
D
Titer (mg/L)
A/a
A/b
B/a
B/b
Culture duration (day)
E
Glucose (g/L)
A/a
A/b
B/a
B/b
Culture duration (day)
F
Lactate (mg/L)
A/a
A/b
B/a
B/b
Culture duration (day)

Figure 1

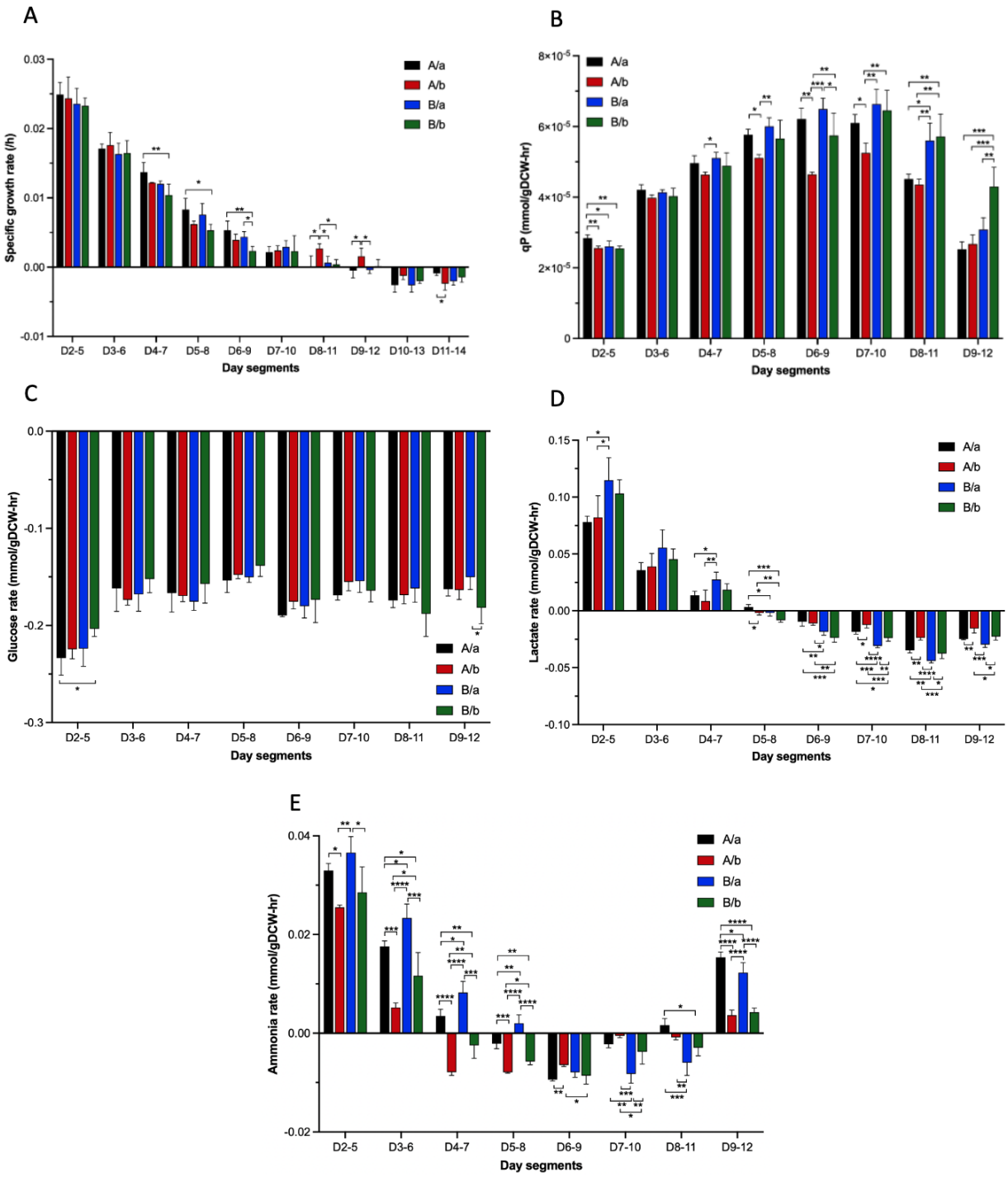

599

600 Figure 2

601

602

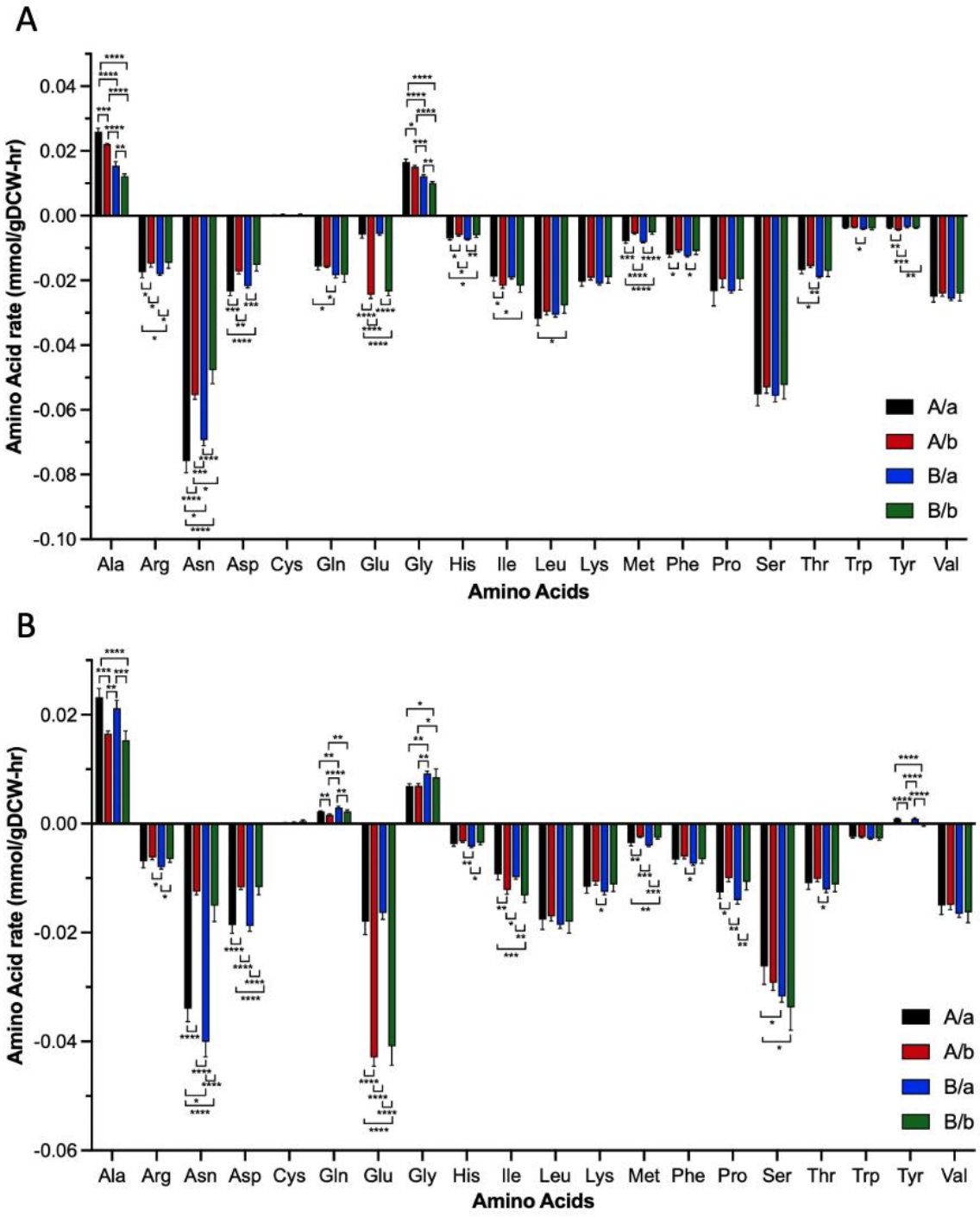

603
604 Figure 3

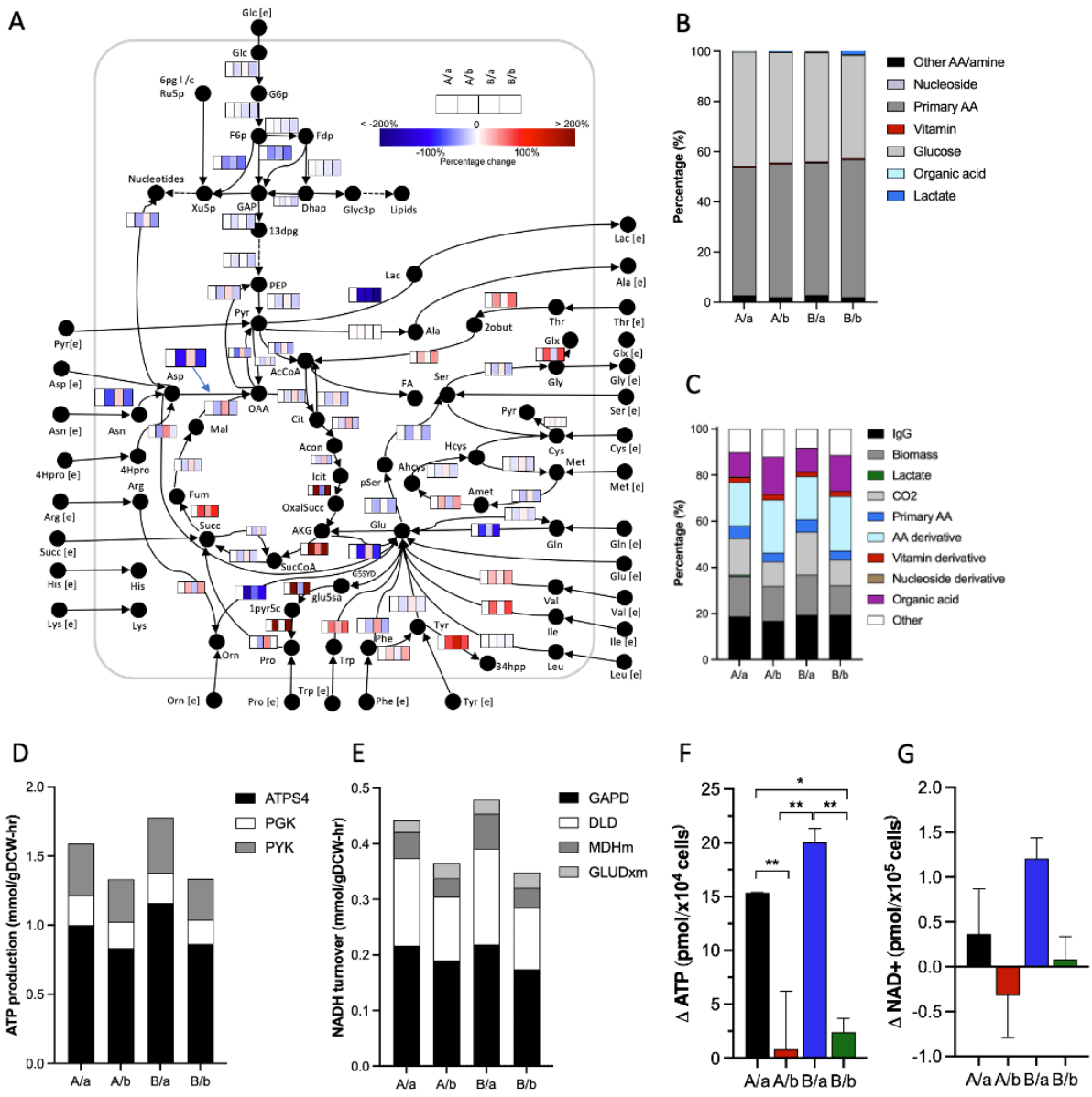
A
B
C
D
E
F
G
Glc [e]
Glc
6pg l /c
Ru5p
G6p
F6p
Fdp
Nucleotides
Xu5p
GAP
Dhap
Glyc3p
Lipids
13dpg
PEP
Pyr
Lac
Ala
2obut
Thr
Glx
Gly
Ser
FA
AcCoA
OAA
Cit
Mal
Acon
Icit
OxalSucc
Fum
Succ
AKG
SucCoA
Glu
Gln
Asp
Asn
4Hpro
Arg
Ahcys
Hcys
Cys
Met
Amet
pSer
Val
Ile
Leu
34hpp
Tyr
Phe
Trp
Pro
Orn
1pyr5c
glu5sa
GSSYD
His
Lys
Pyr[e]
Asp [e]
Asn [e]
4Hpro [e]
Arg [e]
Succ [e]
His [e]
Lys [e]
Lac [e]
Ala [e]
Thr [e]
Glx [e]
Gly [e]
Ser [e]
Cys [e]
Met [e]
Gln [e]
Glu [e]
Val [e]
Ile [e]
Leu [e]
Orn [e]
Pro [e]
Trp [e]
Phe [e]
Tyr [e]
A/a
A/b
B/a
B/b
< -200%
0
> 200%
-100%
100%
Percentage change
Percentage (%)
Other AA/amine
Nucleoside
Primary AA
Vitamin
Glucose
Organic acid
Lactate
IgG
Biomass
Lactate
CO2
Primary AA
AA derivative
Vitamin derivative
Nucleoside derivative
Organic acid
Other
ATP production (mmol/gDCW-hr)
ATPS4
PGK
PYK
NADH turnover (mmol/gDCW-hr)
GAPD
DLD
MDHm
GLUDxm
Δ ATP (pmol/x10^4 cells)
Δ NAD+ (pmol/x10^5 cells)

Figure 4

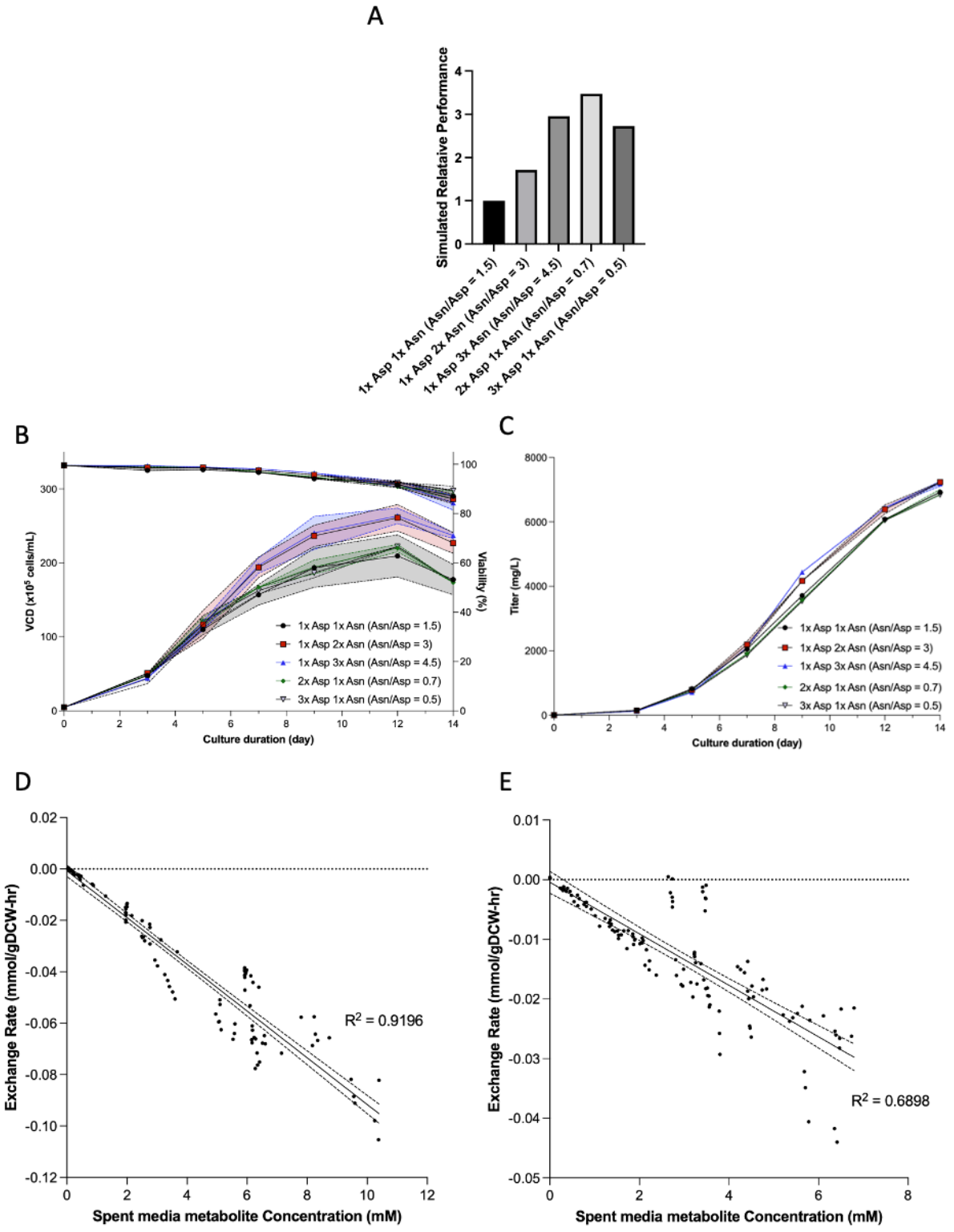
A
Simulated Relataive Performance
1x Asp 1x Asn (Asn/Asp = 1.5)
1x Asp 2x Asn (Asn/Asp = 3)
1x Asp 3x Asn (Asn/Asp = 4.5)
2x Asp 1x Asn (Asn/Asp = 0.7)
3x Asp 1x Asn (Asn/Asp = 0.5)
B
VCD (x10^5 cells/mL)
Viability (%)
Culture duration (day)
C
Titer (mg/L)
Culture duration (day)
D
Exchange Rate (mmol/gDCW-hr)
R2 = 0.9196
Spent media metabolite Concentration (mM)
E
Exchange Rate (mmol/gDCW-hr)
R2 = 0.6898
Spent media metabolite Concentration (mM)

Figure 5